SEMARAK ILMU PUBLISHING

CFD Letters

Journal homepage:
https://semarakilmu.com.my/journals/index.php/CFD_Letters/index
ISSN: 2180-1363

CFD Analysis of The Heave and Pitch Motion of Hull Model

Sergio Murilo Daruis Rocha Filho[1], Roger Matsumoto Moreira[1], Marcio Zamboti Fortes[1,*], Rafael Eitor dos Santos[1]

[1] Engineering School, Industrial Design Laboratory, Fluminense Federal University, Rua Passo da Pátria, 156, D block, room 563A, Niterói, RJ, CEP 24210-240, Brazil

ARTICLE INFO

Article history:
Received 14 February 2022
Received in revised form 19 March 2022
Accepted 29 March 2022
Available online 30 April 2022

Keywords:
Ship motions; RAO; Hull; Sea waves; Computational Fluid Dynamics (CFD)

ABSTRACT

This work aims to predict numerically the vertical motions (heave and pitch) of a Wigley ship model heading over regular waves at Campos Basin, Brazil. Critical levels of periods and amplitudes from waves are determined based on historical data, these are re-dimensioned to a small scale and used as input data to the model. The flow is assumed to be incompressible and viscous with mass and momentum fluxes being conserved. The Computational Fluid Dynamics (CFD) software ANSYS Fluent which makes use of the finite volume method (FVM) is employed to solve continuity and the unsteady Reynolds Averaged Navier-Stokes (RANS) equations with a Shear-Stress Transport (SST) κ-ω turbulence model. The air-water interface is modelled via the Volume of Fluid (VOF) method. An UDF (User Defined Function) is set to simulate only these two degrees of freedom for the ship motion and different sea conditions are simulated with Response Amplitude Operators (RAOs) being compared to experiments, with a good agreement being found. The Campos Basin wave from the Southwest direction with a 1-year occurrence period is a wave with the highest dimensionless value resulting in a 0.172 of heave and the wave that has a North direction with a 1-year occurrence period is a wave with the highest dimensionless value resulting from the 0.097° pitch.

1. Introduction

1.1 Purpose and Motivation

Studies related to the sea motions and its interactions with hull's vessels comprise one of the major areas of interest in naval engineering and the offshore industry, especially for Brazil, which has a huge use of ships in military activities, logistical support, and in activities from oil & gas exploration and production.

In the last century, relevant studies were observed in this area when Froude [1], Krylov [2], and others developed mathematical models and experimental studies trying to describe problems of resistance to the advancement and the ship's behavior in the open sea. From 1950 onwards, a relevant focus was directed to the study of the ship's behavior, both in the open sea and in shallow

* *Corresponding author.*
E-mail address: mzamboti@id.uff.br (Marcio Zamboti Fortes)

https://doi.org/10.37934/cfdl.14.4.1431

waters to develop mathematical models that could describe the actions of the hydrodynamic forces on vessels and the equations of the motion.

The continuous research for mathematical models and motion equations to describe the hydrodynamic forces acting on ships resulted in the publication of papers from Tasai [3] and Ogilvie and Tuck [4]. Vossers *et al.,* [5] tested the hull models from the 60's Series using one wave height and five different wavelengths. Borodai and Netsvetayeve [6] went deeper into the study of heave and pitch movements, while Salvesen, Tuck, and Faltinsen [7] also covered equations of movements in the horizontal plane. Nakamura and Naito [8] tested the propulsion and resistance of a container ship in regular and irregular waves.

The literature shows that several researchers have been investigating the movements of vessels induced by waves using different hulls and wave conditions. Journée [9] carried out experiments to determine the vertical movements for 4 different models of the Wigley hull, under the influence of various wavelengths and wave amplitudes. Shigemi and Zhu [10] comment that most projects of vessels use known environmental loads for convenience, however, the real sea conditions faced by these vessels in their operating locations are different from those considered at the design stage.

Dalane [11] mentions that, when designing offshore structures such as an oil and gas platform, safety is an important part of the process, being essential that the structure can support all the loads acting on it. To ensure that the structural design is within the safety level approved by the authorities, the designer must ensure that the design complies with rules and regulations for the location where a structure will be installed. The traditional methods of ship design have been using experimental studies with test tanks and models of vessels built on a small scale, which require a considerable amount of time and costs to be able to design, assemble, test, and maintain.

Until the development of hardware and software capable of solving the Navier-Stokes equations, the solutions proposed by mathematicians, physicists and engineers were restricted to approximations. With technological advances from computers with greater processing capacity, the use of Computational Fluid Dynamics - CFD techniques has become an important tool for predicting the movements of a ship under the influence of sea loads. The application of the CFD will require only hardware and software whereas the traditional experimental model will require a large infrastructure such as: a laboratory with ample space, test tanks, models of vessels, sensors, hardware, software, and personnel, then the CFD has become a favorable alternative from the financial and deadlines point of view.

Weymouth *et al.,* [12] carried out simulations using a computational code to solve the RANS equations and predict the heave and pitch movements of a Wigley hull for a specific number of Froude, different wave lengths, and different wave amplitudes. The authors Yan *et al.,* [13] applied CFD tools to predict heave and pitch movements also for a Wigley hull while the authors Zhu *et al.,* [14] the movement of the roll. Ghasemi *et al.,* [15] investigated the heave and pitch movements of a Wigley hull and two other forms of the hull (S60 and DDG) by modifying the strip theory using the Maxsurf © software.

Chen *et al.,* [16] simulated the waves generated around a moving Wigley vessel by solving the RANS equations with the κ-ε turbulence model and the Volume of Fluid (VoF) method for the free surface. Mousavi, Khoogar, and Ghasemi [17] present a CFD simulation of a DTMB 5415 ship model with four degrees of freedom using the unsteady RANS method. Nasseroleslami, Sarreshtehdari, and Salari [18] investigated the hydrodynamic pressure field caused by a ship oil tanker using CFD to solve numerically the governing equations including the continuity equation, the momentum equations, and the K-ε turbulence model.

The development of methodologies capable of simulating real parameters, even on small scale, in a virtual environment is one of the most interesting subjects of research related to hull designs.

The design of a hull is a complex task that involves the application of different engineering disciplines, mostly, based on the rules of a ship Classification Society. The ships are designed and built to operate for an average of 20 years, which leads to a great susceptibility for these structures to experience undesired effects due to the motions arising from sea conditions. Drilling Rigs used in oil and gas industry are composed of Risers that are also subjected to external loads such as wave and current which is a critical factor to these structure due to the potential level of fatigue [19].

The methodologies applied to estimate the effects of waves and currents on hulls are based on these international standards, such as API RP 2Sk [20] and DNVGL-RP-C205 [21], which can induce an overestimation of the forces applied to the structures, since they were not developed with the conditions of the specific environmental loads in Brazil.

The main objective of this article is to evaluate, through Computational Fluid Dynamics (CFD) techniques, the heave and pitch movements introduced by waves and currents from a specific area in Brazil that are well known in the Oil and Gas industry and is called “Bacia de Campos” (Campos Basin). Even though the sea waves are different from location to location the ship motions can be simulated considering the data collected from measurement devices installed in the ocean. From those waves that have the highest energy concentration, waves generated by the wind as highlighted by Zuan [22] it is possible to build a reduced scale simulation to predict the heave and pitch motions.

The wave around the hull produces resistance according to the generated wave that has interaction as per Ali [23]. Stappenbelt [24] states that a simplified approach, using simulation which does not analyze the full hydrodynamic complexity from the 6 degrees of freedom also provides a clear indication of floating structure performance trends. Figure 1 illustrates the heave and pitch motions.

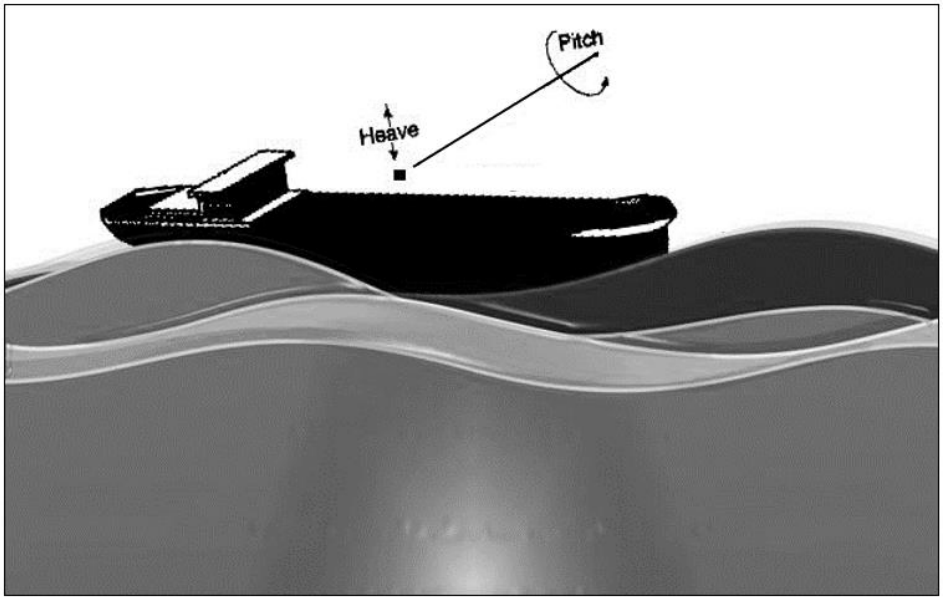

Fig. 1. Heave and pitch motions

Sahak, Sidik and Yusof [25], mention that several characteristic must be taken in consideration when performing a simulation of fluid flow and the development of models with numerous discretization points with the resolution of complex algebraic systems hence special iterative solvers also highlighted by Gomaa and Kasem [26].

In this study was applied the Computational Fluid Dynamics (CFD) software ANSYS Fluent which makes use of the Finite Volume Method (FVM) is employed to solve continuity and the unsteady Reynolds Averaged Navier-Stokes (RANS) equations with a Shear-Stress Transport (SST) κ-ω

turbulence model. The air-water interface is modeled via the Volume of Fluid (VOF) method. An UDF (User Defined Function) has been used to simulate only these two degrees of freedom (heave and pitch) for the ship motion. Different sea conditions are simulated with Response Amplitude Operators (RAOs) being compared to experiments [27].

2. Methodology

2.1 Problem Overview

Different methodologies can be used to predict vessel movements in the six degrees of freedom (6DOF): surge, sway, heave, yaw, pitch, and roll. This work aims to focus on the prediction of the heave and pitch motions illustrated in Figure 2.

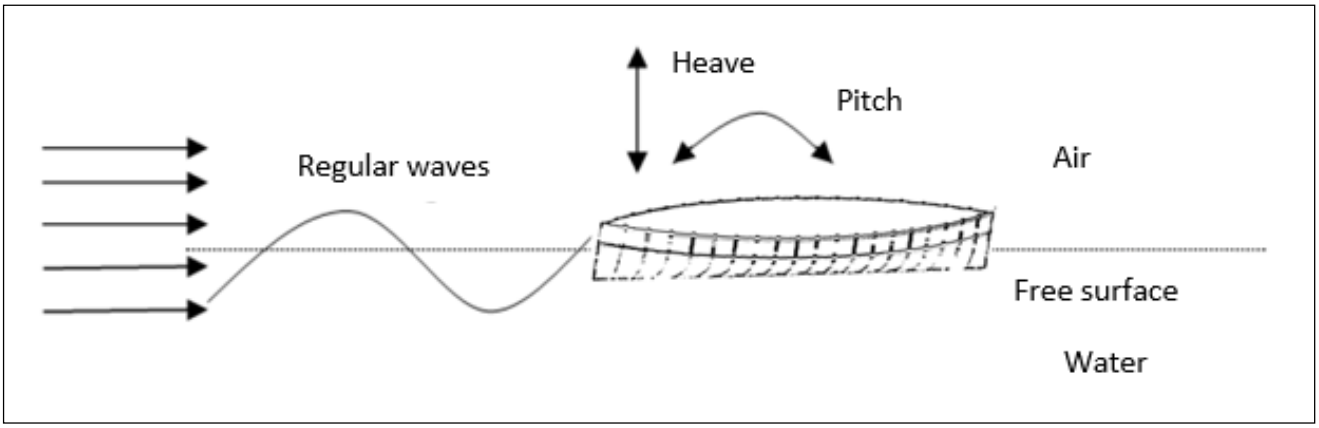

Fig. 2. Study Case

Heave is defined as a vertical translation movement that, positively or negatively, causes a change in the displacement volume. The heave movement means that the ship loses its floating stability then regains it by gravity forces. Pitch is defined as a rotation movement that causes instantaneous variations of trim (inclination of the body) and with this, variations in the distribution of the submerged volume.

The remaining four degrees of freedom: surge, sway, roll, and yaw were kept fixed by an external User Defined Functions - UDF inserted in the ANSYS Fluent© software. The hull applied in this is study is the Wigley III ship model heading over regular waves, which means that the free surface is composed of two fluids: air and water.

Flows that occur around bodies immersed in fluids without boundaries (physical wall limitations) are defined as external flows. External flows are influenced by the Froude Number (Fr), which is a dimensionless parameter that represents the ratio between the forces of inertia and gravitational. This parameter is used in this study to estimate the hydrodynamic performance of the vessel, calculated using Eq. (1).

$$Fr = \frac{U}{\sqrt{gL}} \tag{1}$$

In Eq. (1), the variable U (m/s) is the flow velocity; g (m/s²) is the acceleration due to gravity; L (m) is the length of the vessel under study and Fr is a parameter considered in the calculations of stability and hydrodynamic performance of the vessel. The model used in this work was previously validated through the simulation of input data used in an experiment published by Journée [9].

According to the variable ak given by Journée [9], where the amplitude of the incident wave is a and the number of the wave is k, the heave and pitch movements were simulated during a period of 14 seconds for Froude Number Fr = 0.2. All simulations were performed with constant amplitude a as given by Journée [9], so only the variation in the wavelength changes the ak.

The wave number k was given by Eq. (2).

$$k = \frac{2\pi}{\lambda} \tag{2}$$

The heave movement is represented by z_a which is measured in meters and $z_a^{"}$ which does not have a unit of measure.

$$z_a^{"} = \frac{z_a}{a} \tag{3}$$

The pitch movement is presented by θ_a which is measured in degrees and $\theta_a^{"}$ that does not have unit of measure.

$$\theta_a^{"} = \frac{\theta_a}{360}\frac{L}{a} \tag{4}$$

The variables $z_a^{"}$ and θ_a were obtained by calculating the vertical oscillation center.

$$z_a = Z_{max} - Z_{min} \tag{5}$$

$$\theta_a = \theta_{max} - \theta_{min} \tag{6}$$

The value of Z_{max} and θ_{max} are the maximum value of Z e θ in the simulated period. The Z_{min} and θ_{min} are the minimum value of Z e θ in the simulated period. The dynamic response from a range of frequencies with a unique wave amplitude related to a floating structure is known as Response Amplitude Operators (RAO).

Regarding the movement of the hull under the influence of regular waves, the RAO represents a transfer function, for a given wave frequency. In this study, the RAO is measured from the responses of a floating structure to waves with different characteristics. Considering the conditions simulated in this study, Eq. (7) and Eq. (8) expose the analytical expressions for each of the RAOs evaluated in the time domain:

$$\zeta = \zeta_{max}\cos(\Omega_z t + \phi_z) \tag{7}$$

$$\Theta = \Theta_{max}\cos\left(\Omega_y t + \phi_y\right) \tag{8}$$

The variables ζ and Θ represent the heave and the pitch. The parameters ζ_{max} and Θ_{max} are the amplitudes of each movement; Ω_z and Ω_y are the angular frequencies in rad/s; ϕ_z and ϕ_y are the corrections for vertical translation and rotation around the transverse axis in radians. The critical levels of periods and amplitudes from waves that occur in Campos Basin are determined based on historical data extracted from a technical specification from CENPES [28].

Table 1 presents: Hs (m) is the significant height, TPHs (s) is the period of significant height, HMAX (m) is the maximum height, TPHMAX (s) is the period of maximum height and U (m/s) is the current. The value of the wavelength represented by λ (m) exposed in Table 1, was calculated for each wave direction based on the period (s) associated with the significant height.

Table 1
Wave directions and parameters

Wave direction	Wave period (years)	Hs (m)	TPHs (s)	U (m/s)	λ (m)	k (m^{-1})	a	ak
Southwest(SW)	1	6.37	13.93	1.47	302.96	0.021	3.185	0.066
South (S)	100	7.1	14.35	2.06	321.51	0.02	3.55	0.069
East (E)	100	4.87	10.4	1.13	168.87	0.037	2.435	0.091
West and Northwest (W-NW)	100	3.88	8.51	1.26	113.07	0.056	1.94	0.108
Southeast (SE)	10	5.72	10.28	1.62	165	0.038	2.86	0.109
Northeast (NE)	1	4.55	9.13	0.81	130.15	0.048	2.275	0.11
North (N)	1	4.44	8.81	1.12	121.18	0.052	2.22	0.115

Table 1 details the selected waves in the Campos Basin considering the ak, or slope of the wave, of the highest value for each direction. The wavelength λ (m) and the amplitude of wave a were scaled to a reduced scale, enabling computational simulation.

2.2 Governing Equations

The unsteady incompressible and viscous flow with a free surface is modeled in three dimensions with momentum and mass being conserved in the fluid domain [29]. Continuity and the unsteady RANS equations are satisfied.

$$\frac{\partial \bar{u}_i}{\partial x_i} = 0 \tag{9}$$

$$\frac{\partial \bar{u}_i}{\partial t} + \frac{\partial \left(\bar{u}_i \bar{u}_j\right)}{\partial x_j} = f_i - \frac{1}{\rho}\frac{\partial \bar{P}}{\partial x_i} + \nu \frac{\partial^2 \bar{u}_i}{\partial {x_j}^2} - \frac{\partial}{\partial x_j}\overline{u_i{}' u_j{}'} \tag{10}$$

where the subscript i indicates the direction of an orthogonal axes system; t is time; x_i is the position; $u_i = \bar{u}_i + u_i^{'}$ is the fluid velocity decomposed, respectively, in mean and fluctuating velocities; $f_i = (0.0. -g)$ is the acceleration due to gravity; ρ is the fluid density; $\bar{P}$ is the mean dynamic pressure; ν is the kinematic viscosity.

2.3 Turbulence Model

The shear stress transport $k - \omega$ turbulence model, proposed by Menter [30], is used to solve the closure problem.

$$\frac{\partial(\rho\kappa)}{\partial t} + \frac{\partial(\rho\kappa u_i)}{\partial x_i} = P_\kappa - \beta^* \rho\omega\kappa + \frac{\partial}{\partial x_i}\left[(\mu + \sigma_\kappa \mu_t)\frac{\partial \kappa}{\partial x_i}\right] \tag{11}$$

$$\frac{\partial(\rho\omega)}{\partial t} + \frac{\partial(\rho\omega u_i)}{\partial x_i} = \rho\alpha S^2 - \rho\beta\omega^2 + \frac{\partial}{\partial x_i}\left[(\mu + \sigma_\omega \mu_t)\frac{\partial \omega}{\partial x_i}\right] + 2(1 - F_1)\sigma_d \frac{\rho}{\omega}\frac{\partial \kappa}{\partial x_i}\frac{\partial \omega}{\partial x_i} \tag{12}$$

where k is the turbulent kinetic energy; ω is the rate of dissipation of the eddies; μ is the molecular viscosity; μ_t is the turbulent viscosity. The term S and Sij are below defined.

$$S = \sqrt{2\overline{S_{ij}S_{ij}}} \tag{13}$$

$$S_{ij} = \frac{1}{2}\left(\frac{\partial u_i}{\partial x_j} + \frac{\partial u_j}{\partial x_i}\right) \tag{14}$$

The term P_κ is defined by Eq. (15).

$$P_\kappa = min\left(\mu_t \frac{\partial u_i}{\partial x_j}\left(\frac{\partial u_i}{\partial x_j} + \frac{\partial u_j}{\partial x_i}\right) \rightleftarrows \rightleftarrows \; ; \; 10\beta^*\omega\kappa\right) \tag{15}$$

and the term F_1 is defined by Eq. (16).

$$F_1 = tanh\left\{\left\{min\left(max\left(\frac{\sqrt{\kappa}}{\beta^*\omega y} \; ; \; \frac{500\nu}{y^2\omega}\right) \; ; \; \frac{4\rho\sigma_{\omega 2}\kappa}{CD_{\kappa\omega}y^2}\right)\right\}^4\right\} \tag{16}$$

where y is the non-slipping distance, and $CD_{\kappa\omega}$ is defined by Eq. (17)

$$D_{\kappa\omega} = max\left(2\rho\sigma_{\omega 2}\frac{1}{\omega}\frac{\partial\kappa}{\partial x_i}\frac{\partial\omega}{\partial x_i} \; ; \; 10^{-10}\right) \tag{17}$$

The other constants are: β = 0.075; β* = 0.09; σ_k = 0.5; σ_ω = 0.5; σ_d = 0.856; a = 5/9.

2.4 Interface Air-Water Model

Air-water interface is modeled via the VOF - Volume of Fluid method, proposed by Hirt and Nichols [31].

$$\frac{\partial\Phi}{\partial t} + u_i \cdot \nabla\Phi = 0 \tag{18}$$

where Φ represents the volume fraction of the liquid phase, $0 \leq \Phi \leq 1$.

2.5 Finite Volume Method

The computational fluid dynamics code ANSYS Fluent © uses the Finite Volume Method (MVF). Four steps are performed: discretization of the fluid domain in control volumes, application of the conservation equations in each volume, approximation of the derivatives in the applicable equations in linear terms, and solution of the linear equations by an iterative method.

The unknowns of the problem are solved in the centroid of each control volume and inside the balance of the variables is preserved. The selection of linear approximation models must be made taking into account the characteristics of the transport phenomenon involved.

2.6 Computational Model

Fluid dynamics techniques have experienced great advances through the development of computers with greater capacity for processing numerical simulation of any physical or chemical process. In this work, the real and continuous problem of the movement of vessels discretized in the domain in finite volumes is approached. The simulation is based on the principles of conservation of energy, mass, and amount of movement. The CFD consists of an accurate forecast of fluid flow through:

I. Mathematical modeling (partial differential equations)
II. Numerical methods (discretization and solution techniques);
III. Tools and software (solvers, pre and post-processing).

2.7 Geometry

The geometry analyzed in this study is the reduced Wigley III hull model, which was also analyzed in the works by Journée [9], Yan *et al*., [13] Ghasemi *et al.,* [15], and Chen *et al.,* [16]. Figure 3 presents the Wigley III hull model.

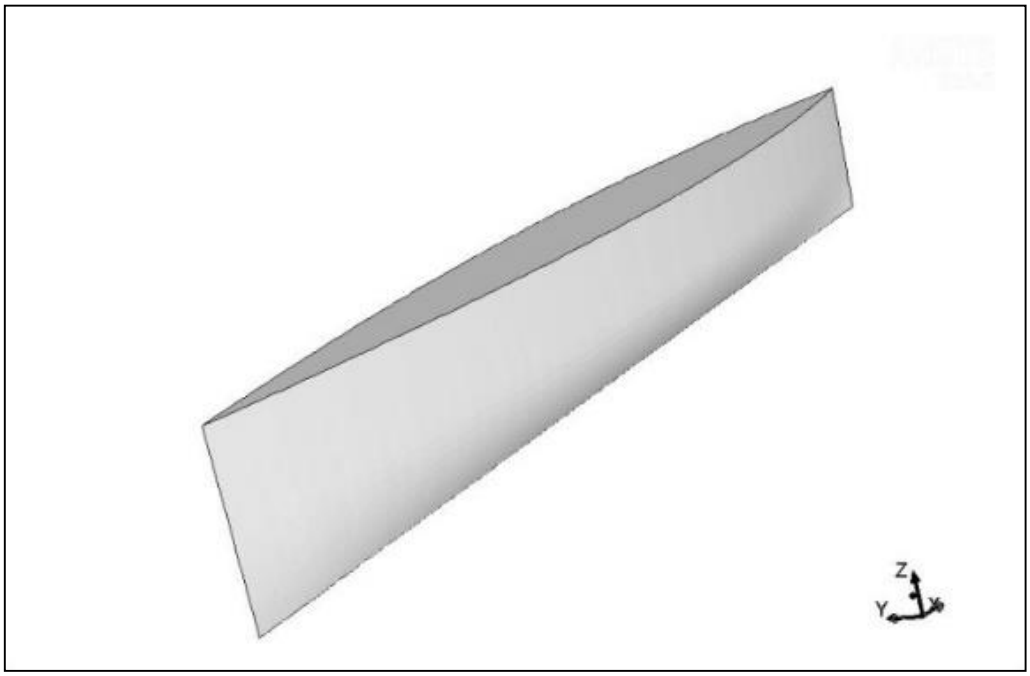

Fig. 3. Wigley III hull model

Table 2
presents the main design data from the hull

Main data from hull	Values
Amidships section coefficient, C_m	0.6667
Length to breadth ratio, *L/B*	10.0
Length, *L* (m)	2.3600
Breadth, *B*(m)	0.3000
Draught, *d* (m)	0.1875
Trim, *t* (m)	0.0000
Volume of displacement, V (m3)	0.0780
Center of rotation above base, K R (m)	0.1875
Center of gravity above base, KG (m)	0.1700
Radius of inertia for pitch, Kyy (m)	0.7500

The computational model used in the simulation was similar to a Tank [32] with the following dimensions: length 15m, width 6m, and height 4.5m. Despite the apparent similarity to a tank (Figure 4), the model is in fact an open channel, because all walls were defined with a damping condition, avoiding the reflection of the waves.

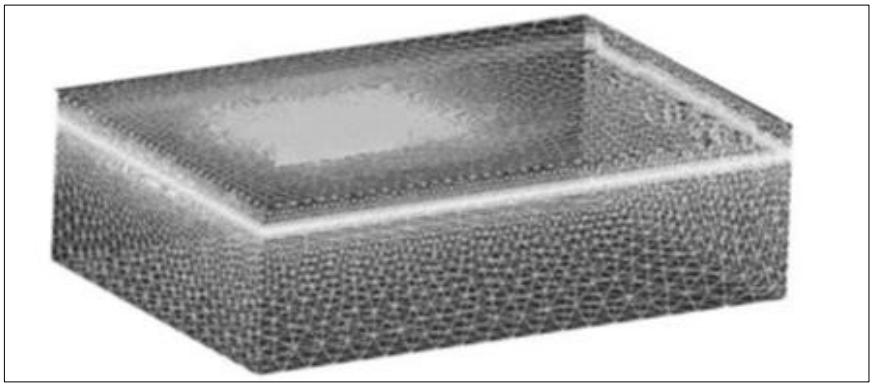

Fig. 4. Model similar to tank but with open channels

According to Yanuar *et al.,*[29], prismatic meshes generate better results than tetrahedral meshes in free surface regions. Therefore, unstructured prismatic meshes (see Figure 5) were used in the vicinity of the air-water interface and unstructured tetrahedral meshes in the other regions [33].

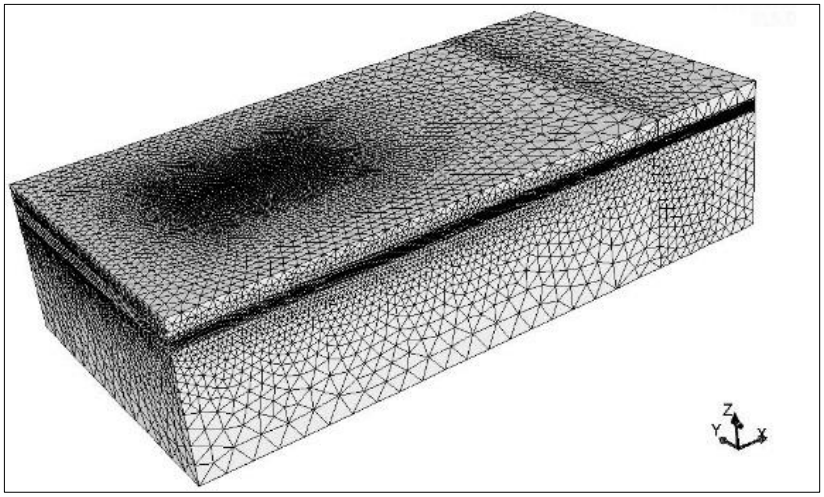

Fig. 5. Mesh

2.8 Boundary Conditions

Boundary conditions (see Figure 6 and Table 3) give the solution found by the CFD method a unique character, dictating how the solver addresses the problem and interprets the various geometries involved.

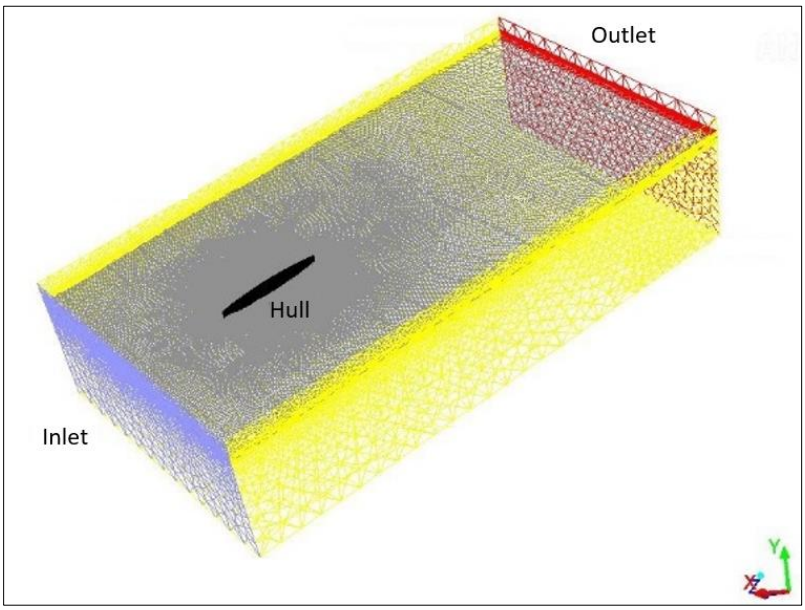

Fig. 6. Boundaries

The flow in the liquid phase is defined in the positive direction of the longitudinal direction in the "Input", with the regular waves generated at the level of the air-water interface, the average value of 0.02 meters was adopted for the one obtained from the amplitudes resulting from the experiment by Journée [9], therefore the height was fixed at 0.04 meters and the wavelength changed according to each simulation performed.

The "Exit" was considered an open channel, with a pressure specified at the level of the air-water interface. The entire air phase was treated with a constant pressure equal to 1 atm. The side walls were defined with a damping condition so that there was no reflection of the waves. The bottom of the fluid domain and the reduced hull model were treated with conditions of impenetrability and non-slip.

Table 3
Boundaries

Boundary name - condition	Position
inlet - velocity	x=4.5m
outlet - outflow	x=6.5m
port side - symmetry	y=3.0m
starboards side - symmetry	y=-3.0m
up - symmetry	z=1.5m
down - symmetry	z=-3.0m
the hull - no-slip wall	-

2.9 Validation of the Case in Study

The model used in this work was previously validated through the simulation of input data used in an experiment published by Journée [9]. All simulations were performed and the ship motions of heave and pitch for a Wigley-III model were reproduced numerically and validated with experiments (see Figure 7 and Figure 8) carried out by Journée [9].

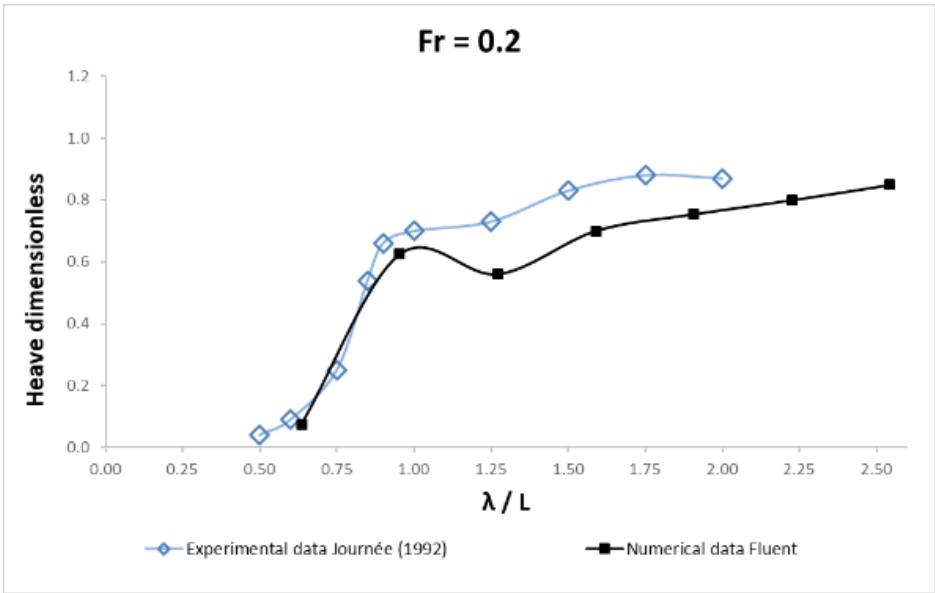

Fig. 7. Heave from Numerical data fluent versus Experimental data Journée [9]

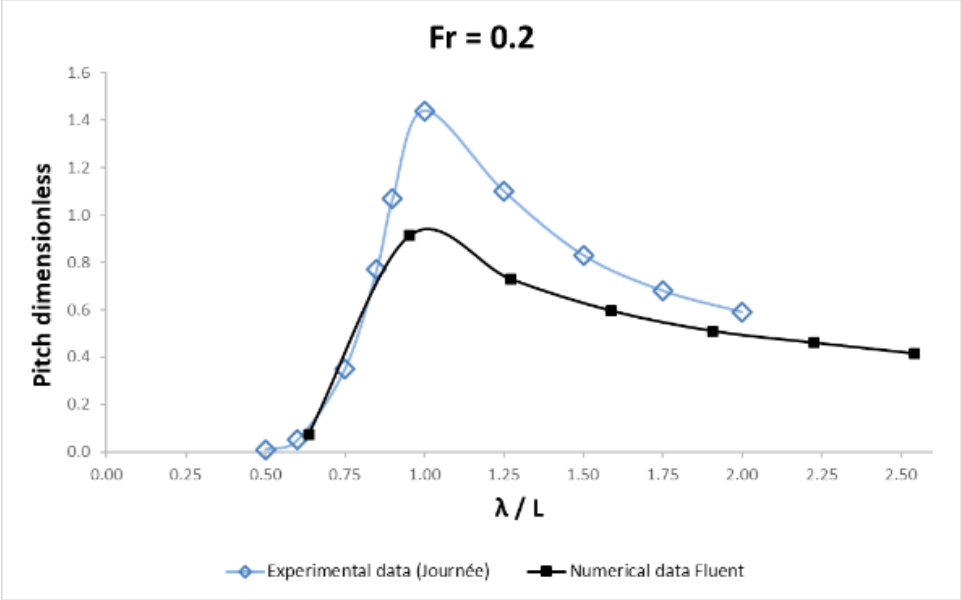

Fig. 8. Pitch from Numerical data fluent versus Experimental data Journée [9]

A good agreement is found between experimental and numerical results except for $1.0 < \lambda/L \leq 1.25$ for Fr = 0.2. Sea conditions with wave lengths similar to the size of the hull cause high changes in the vertical orientation of the ship model.

3. Results

In this work, heave and pitch motions forced by waves and currents from the Campos Basin were evaluated using computational fluid dynamics (CFD) techniques for a Wigley III hull model.

The periodic behavior of the waves was observed after the initial three seconds due to the formation of a transient in the fluid domain. This trend happened for both heave and pitch simulations, as shown in Figures 9 and 10 respectively. The selection criterion used to determine the period of interest was based on the use of ΔT ≥ 4 (s); $Z_{max} \leq$ 0.00159 (m) and $Z_{min} \geq$ - 0.00141 (m) for heave; $\theta_{max} \leq$ 0.22 (°) and $\theta_{min} \geq$ - 0.23 (°) for pitch.

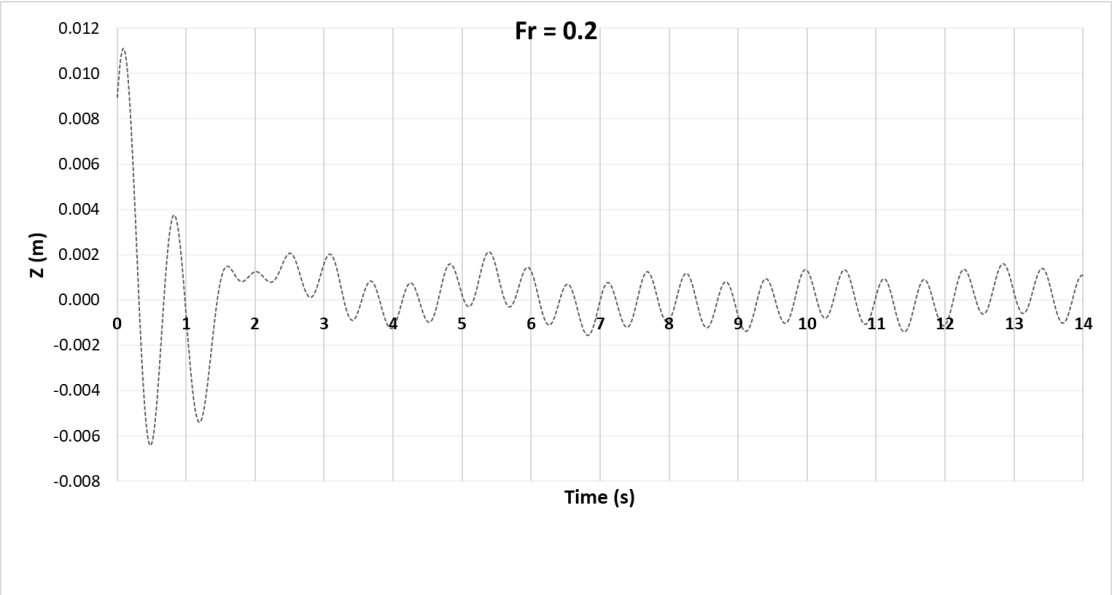

Fig. 9. Simulation of 14 seconds for heave movement

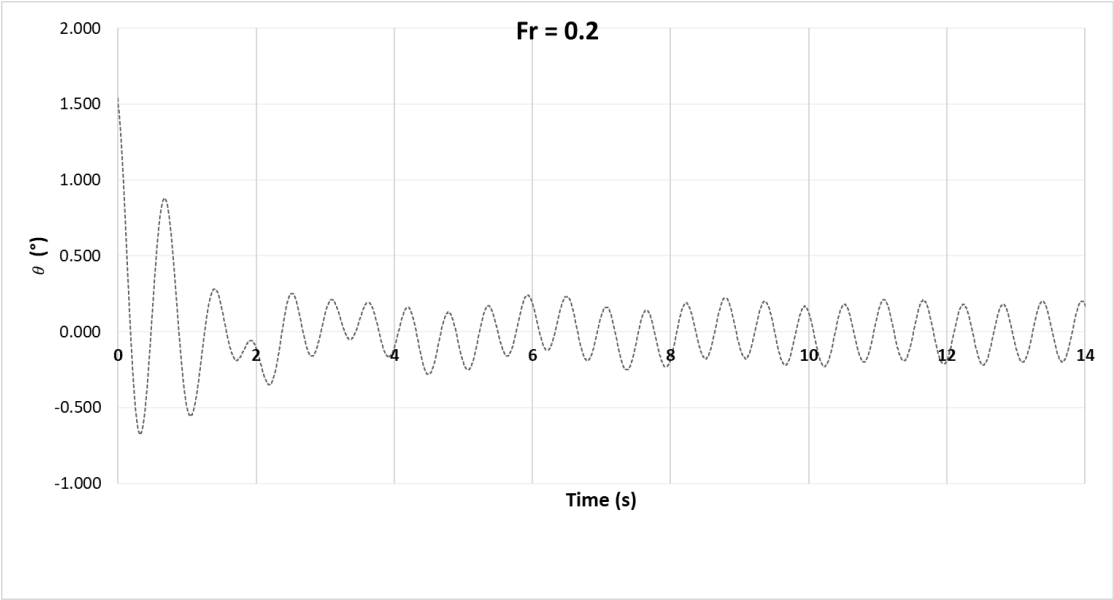

Fig. 10. Simulation of 14 seconds for the pitch movement

Figure 11 presents the heave results for each simulation scenario of ak and λ / L > 0.5.

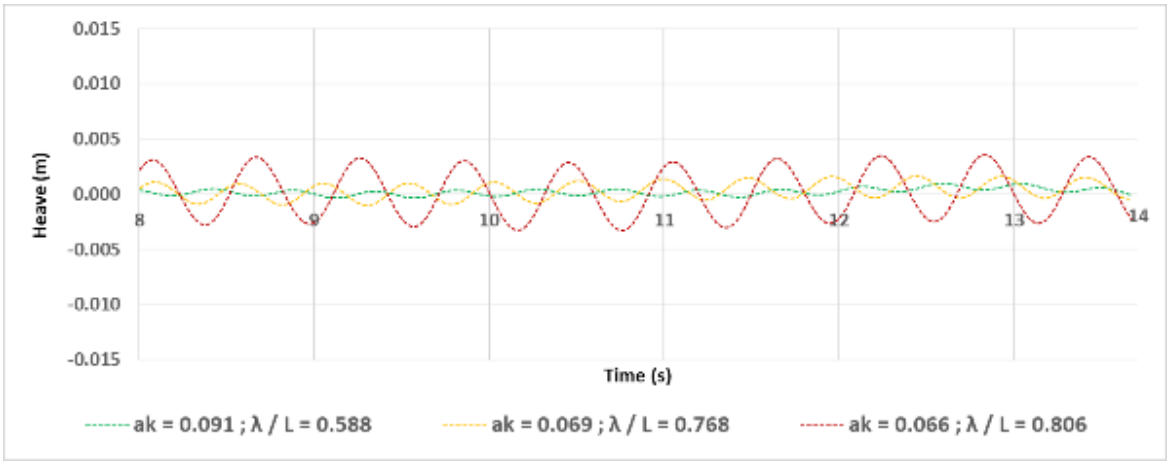

Fig. 11. Heave results for λ / L > 0.5

As presented in Figure 11 the λ / L = 0.588 where the wavelength is above, however, still close to half the length of the vessel, the movement relative to the heave tends to be less, with the peak value below 0.001 meters. For the simulation of λ / L = 0.768, the value in meters of the heave exceeded 0.001 after 10 seconds. In both cases, 0.588 and 0.768, a similar behavior is observed in terms of frequency, since there is the formation of at least 3 peaks and 3 valleys every second, with spacing from peak to peak being similar.

For λ / L = 0.806, a lower frequency is noted, but the amplitude of the heave is considerably greater than the other two λ / L analyzed in this group. The peak value for this λ / L exceeded 0.003 meters.

Table 4
Calculated RAO of heave results under λ / L > 0.5

U (m/s)	λ (m)	λ / L	ak	ζa
1.13	1.39	0.588	0.091	0.032
2.06	1.81	0.768	0.069	0.066
1.47	1.90	0.806	0.066	0.172

Comparing these three results, it is possible to see the Campos Basin wave from the Southwest direction and a 1-year occurrence period is a wave with the highest dimensionless value resulting in a 0.172 of heave (see Table 4)

The Figure 12 presents the heave results of λ / L < 0.5.

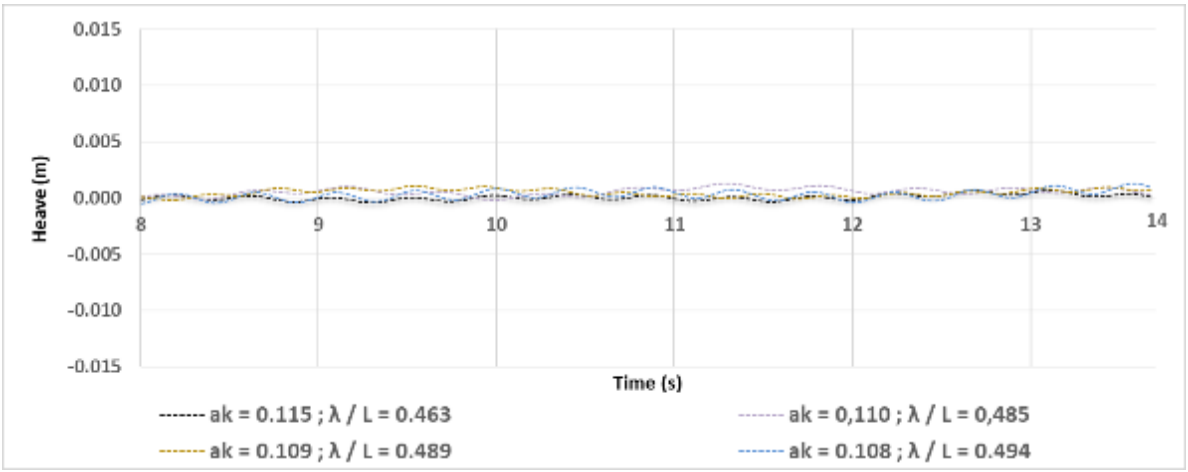

Fig. 12. Heave results for λ / L < 0.5

All λ / L presented in the graph have values below 0.5, which means that the wave length is less than half the length of the vessel, therefore, the heave values tend to be relatively low. The peak values found for these cases were around 0.001 meters.

There is a significant difference between the frequencies presented for each λ / L, the current variation being one of the possible influences on this wave behavior. As the value of the length from these waves obtained a small variation, the behavior shown in Figure 12 corroborates the expected result for this simulation.

Between seconds 12 and 13 can be seen three of the four cases with similar peak-to-peak values, except for λ / L = 0.485. In the latter case, the peak value was the highest in this group, being the only one to exceed the value of 0.001 meters. Table 5 shows the respective RAO values for this group of simulations.

Table 5
Calculated RAO of heave results under λ / L < 0.5

U (m/s)	λ (m)	λ / L	*ak*	ζa
1.12	1.09	0.463	0.115	0.028
0.81	1.14	0.485	0.110	0.037
1.62	1.15	0.489	0.109	0.031
1.26	1.17	0.494	0.108	0.045

When comparing these four results, can be seen that the Campos Basin wave has a West-Northwest direction and 100-year period of occurrence with the highest wave value for heave resulting in 0.045.

Figure 13 shows the ascending RAO related to heave data versus λ / L

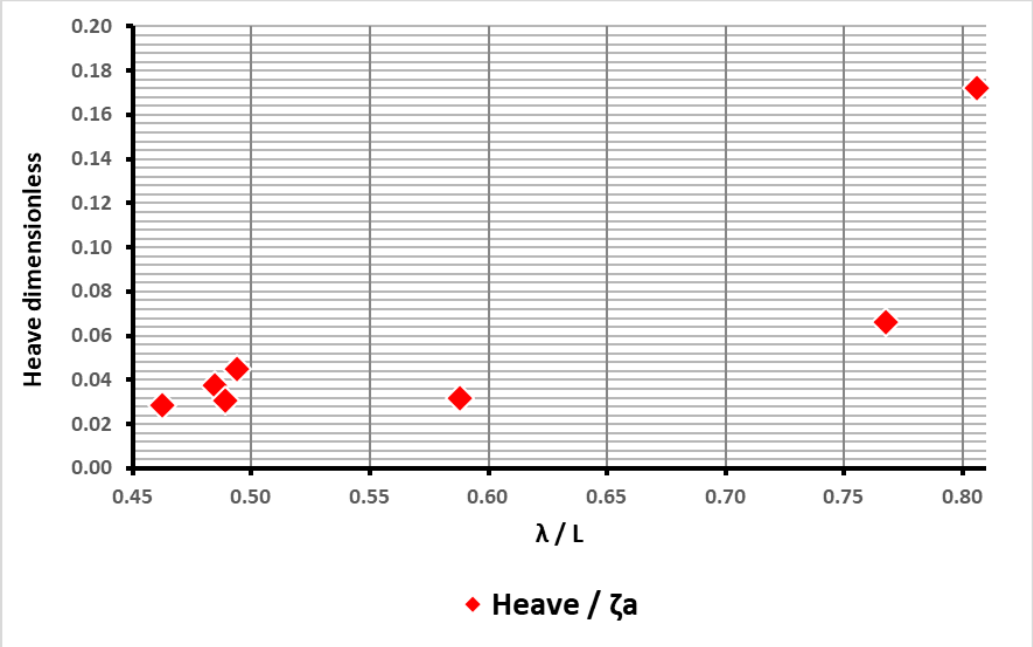

Fig. 13. Heave RAO versus λ / L

The pitch results for cases of λ / L ≥ 0.5 (see Figure 14) followed the same characteristics found in the heave.

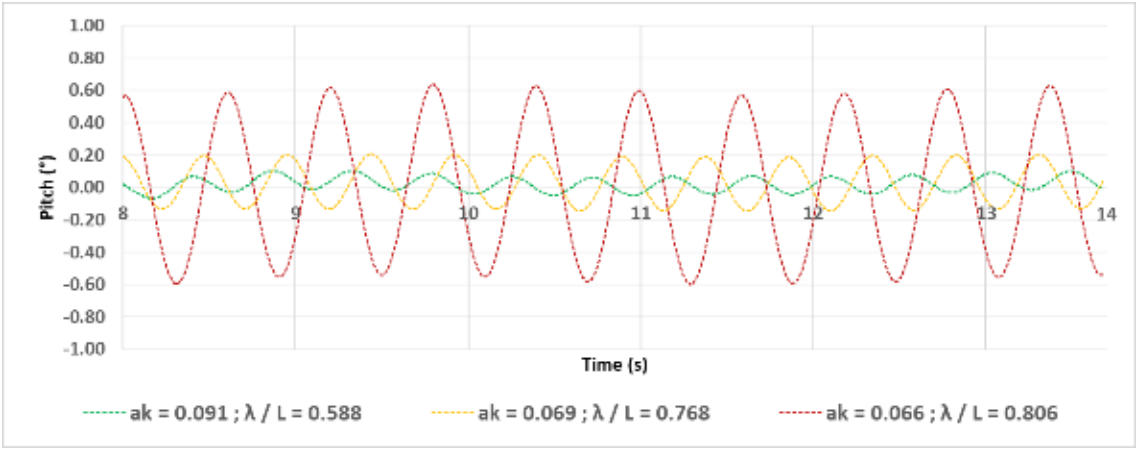

Fig. 14. Group of pitch results for λ / L > 0.5

The most critical case was the λ / L = 0.806, which presented the highest θ peak results, around 0.6°. In the case where the wavelength is close to half the length of the vessel λ / L = 0.588, the relative pitching movement also showed the lowest value, resulting in θ ≈ 0.1°. For λ / L = 0.768 is noted that the peak wave value is around 0.2°. For λ / L = 0.806, the pitch values close to 0.6° were observed. Table 6 shows the respective RAO values for this group of pitch simulations.

Table 6
Calculated RAO of pitch results under λ / L > 0.5

U (m/s)	λ (m)	λ / L	ak	ζa
1.13	1.39	0.588	0.091	0.087
2.06	1.81	0.768	0.069	0.100
1.47	1.90	0.806	0.066	0.402

Comparting these first three results, can be seen that the Campos Basin wave has the Southwest direction and 1year occurrence period with the highest value resulting from 0.402. The following scenarios values of ak were equal to or greater than 0.1 and the λ / L less than 0.5.

The λ / L shown in Figure 15 demonstrate the vessel has a low relative response to pitch under simulated wavelength and hull conditions. The peak values of θ were below 0.2° and a value of -0.2° for all these four simulated cases. It is noticed that of these 4 simulated cases, three of them had similar peak-to-peak values, except for λ / L = 0.489, being the only one to approach the value of 0.2°. Table 7 shows the respective RAO values for this group of pitch simulations.

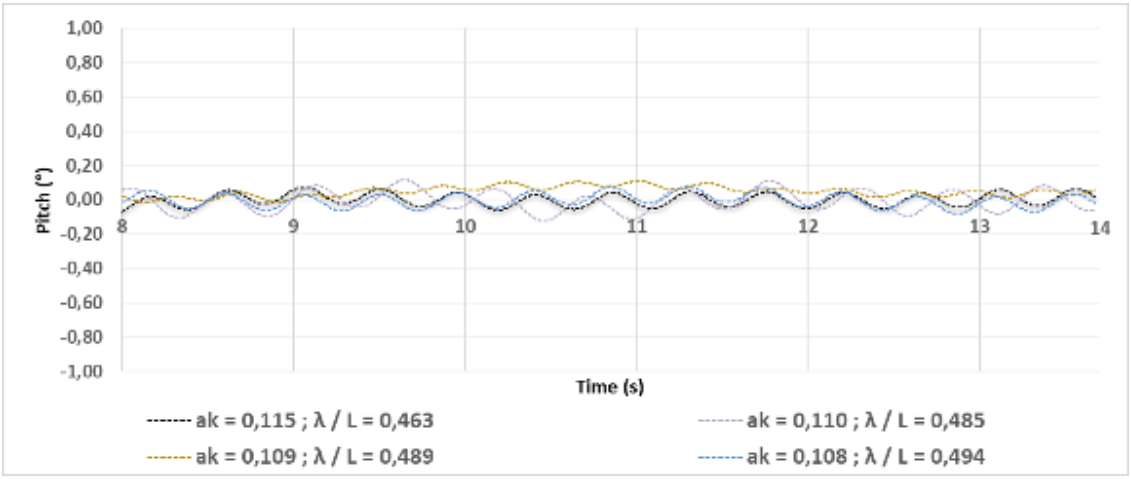

Fig. 15. Group of pitch results for λ / L < 0.5

Table 7
Calculated RAO for the group of pitch results under λ / L < 0.5

U (m/s)	λ (m)	λ / L	ak	ζa
1.12	1.09	0.463	0.115	0.097
0.81	1.14	0.485	0.110	0.048
1.62	1.15	0.489	0.109	0.020
1.26	1.17	0.494	0.108	0.044

Comparing these four results is clear the Campos Basin wave that has a North direction and a 1-year occurrence period is a wave with the highest dimensionless value resulting from the 0.097° pitch. Figure 16 shows the RAO pitch data concerning to λ / L in an increasing way, maintaining the same scales presented in the validation of the model used for simulation.

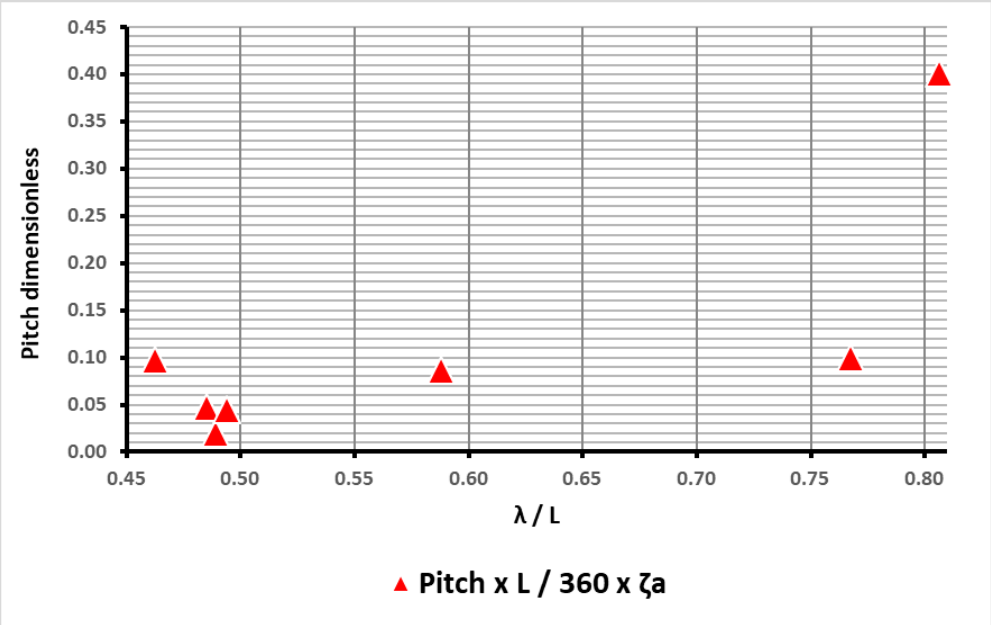

Fig. 16. Pitch RAO versus λ / L

The pitch for the first four points on the graph are λ / L = 0.463; 0.485; 0.489; 0.494 was less than 0.1°, and for the three cases of λ / L ≥ 0.5 there was an upward trend in the curve at these points.

4. Conclusions

In this work, heave and pitch motions forced by waves and currents from the Campos Basin were evaluated using computational fluid dynamics (CFD) techniques for a Wigley III hull model.

The critical levels of wave periods and amplitudes were determined for each direction of the Campos Basin waves, which are simulated on a small scale using the ANSYS Fluent© software. The vessel's responses to sea conditions were measured using the Response Amplitude Operators (RAO). The Finite Volume Method (MVF) was used to solve the mass conservation and momentum equations (Reynolds Averaged Navier-Stokes), with turbulence represented by the κ-ω SST model (Shear Stress Transport) and the Volume method Fluids (VOF) for the analysis of the air-water interface. The calculations and processing were performed using the computational fluid dynamics code ANSYS Fluent© 19.0. with customizations performed via UDF.

The numerical results of this study demonstrate that simulations via CFD can offer a good prediction of RAOs distant from $\lambda / L < 1.0$. Cases in which the incident waves have a length less than that of the hull size $\lambda / L \leq 0.5$ showed precise numerical results, both for heave and for pitch.

Experimental studies can benefit from the numerical results, helping to dimension the experimental apparatus and foresee possible problems. The development of methodologies for simulating real parameters in a virtual environment is of great interest for vessel hull projects, making it possible to evaluate different scenarios with less demand for time and costs. This work is an example of the use of real data from the Campos Basin and the application of this methodology can be expanded to carry out studies on the other regions of Brazil that also have offshore structures or relevant maritime traffic, such as “Bacia do Espirito Santo”, “Bacia de Santos”, “Bacia de Sergipe”, “Bacia de Pernambuco-Alagoas” and others.

Acknowledgment

The authors acknowledge Fluminense Federal University for its educational support and supply of licenses for the ANSYS code. Also, they express appreciation to the reviewers for all remarks and suggestions. This research was not funded by any grant.

References

[1] Froude, William. "On the rolling of ships." *Trans INA* 2 (1861): 180-227.
[2] Kriloff, A. *A new theory of the pitching motion of ships on waves, and of stressed produced by this motion*. Institution of naval Architects, 1896.
[3] Tasai, Fukuzo. "On the damping force and added mass of ships heaving and pitching." *Journal of Zosen Kiokai* 1959, no. 105 (1959): 47-56. https://doi.org/10.2534/jjasnaoe1952.1959.47
[4] Ogilvie, T. F., and E. O. Tuck. "A rational strip theory of ship motions: part 1. Report No 013." *The Department of Naval Architecture and Marine Engineering, The University of Michigan, College of Engineering* (1969).
[5] Vossers, G., W. A. Swaan, and H. Rijken. "Experiments with series 60 models in waves." *International Shipbuilding Progress* 8, no. 81 (1961): 201-232. https://doi.org/10.3233/ISP-1961-88102
[6] Borodai, I. K. and Netsevvetayev, Y. A. “Ship motion in Ocean Waves” *Sudostroenie, Leningrad* (1969).
[7] Salvesen, N., Tuck, E. O. and Faltisen, O. “Ship motions and sea loads”. *Transactions Society Naval Architects Marine Engineers* 78 (1970).
[8] Nakamura, Shoichi, and Shigeru Naito. "Propulsive performance of a container ship in waves." *Journal of the Society of Naval Architects of Japan* 15 (1977).
[9] Journee, Johan MJ. "Experiments and calculations on four Wigley hullforms." *TUDelft, Faculty of Marine Technology, Ship Hydromechanics Laboratory, Report No. 909* (1992).
[10] Shigemi, Toshiyuki, and Tingyao Zhu. "Extensive study on the design loads used for strength assessment of tanker and bulk carrier structures." *Journal of marine science and technology* 9, no. 3 (2004): 95-108. https://doi.org/10.1007/s00773-004-0179-5
[11] Dalane, Eirik. "Estimation of ALS wave-column impact loads for a semi-submersible and a simplified assessment of the associated structural response." Master's thesis, Norges teknisk-naturvitenskapelige universitet, Fakultet for ingeniørvitenskap og teknologi, Institutt for marin teknikk, 2011.
[12] Weymouth, Gabriel David, Robert Vance Wilson, and Frederick Stern. "RANS computational fluid dynamics predictions of pitch and heave ship motions in head seas." *Journal of ship research* 49, no. 02 (2005): 80-97. https://doi.org/10.5957/jsr.2005.49.2.80
[13] Yan, Jiao, Dingqi Pan, Xiaomin Zhou, and Ketai He. "The prediction of ship motions and added resistance based on RANS." In *2015 15th International Conference on Control, Automation and Systems (ICCAS)*, pp. 1978-1982. IEEE, 2015. https://doi.org/10.1109/ICCAS.2015.7364692
[14] Zhu, Ren-chuan, Chun-lei Yang, Guo-ping Miao, and Ju Fan. "Computational fluid dynamics uncertainty analysis for simulations of roll motions for a 3D ship." *Journal of Shanghai Jiaotong University (Science)* 20, no. 5 (2015): 591-599. https://doi.org/10.1007/s12204-015-1666-z
[15] Ghassemi, Hassan, Sohrab Majdfar, and Valiollah Gill. "Calculations of the heave and pitch RAO’s for three different ship’s hull forms." *Science and Engineering* 22 (2015).

[16] Shengtao, Chen, Zhong Jingjun, and Sun Peng. "Numerical simulation of the stokes wave for the flow around a ship hull coupled with the VOF model." *Journal of Marine Science and Application* 14, no. 2 (2015): 163-169. https://doi.org/10.1007/s11804-015-1305-y
[17] Mousavi, S. M., A. R. Khoogar, and H. Ghassemi. "Time Domain Simulation of Ship Motion in Irregular Oblique Waves." *Journal of Applied Fluid Mechanics* 13, no. 2 (2019): 549-559. https://doi.org/10.29252/jafm.13.02.30218
[18] Nasseroleslami, A., A. Sarreshtehdari, and M. Salari. "Numerical Study of the Hydrodynamic Pressure Field Generated due to Ship Motion at Different Speeds." *Journal of Applied Fluid Mechanics* 13, no. 5 (2020): 1575-1586. https://doi.org/10.36884/jafm.13.05.31283
[19] Alias, Fatin, Mohd Hairil Mohd, Mohd Azlan Musa, Erwan Hafizi Kasiman, and Mohd Asamudin A. Rahman. "Flow Past a Fixed and Freely Vibrating Drilling Riser System with Auxiliaries in Laminar Flow." *Journal of Advanced Research in Fluid Mechanics and Thermal Sciences* 87, no. 3 (2021): 94-104. https://doi.org/10.37934/arfmts.87.3.94104
[20] API RP 2Sk *"Design and Analysis of Stationkeeping Systems for Floating Structures", Third Edition, API* (2015).
[21] DNVGL-RP-C205 *"Condições ambientais e cargas ambientais", DNV* (2017).
[22] Zuan, A. M. S., M. K. Z. Anuar, S. Syahrullail, M. N. Musa, and E. A. Rahim. "A study of float wave energy converter (FWEC) model." *Journal of Advanced Research in Applied Sciences and Engineering Technology* 1, no. 1 (2015): 40-49.
[23] Ali, Arifah, Adi Maimun, and Yasser Mohamed Ahmed. "Analysis of Resistance and Generated Wave around Semi SWATH Hull at Deep and Shallow Water." *Journal of Advanced Research in Fluid Mechanics and Thermal Sciences* 58, no. 2 (2019): 247-260.
[24] Stappenbelt, Brad. "Prediction of the heave response of a floating oscillating water column wave energy converter." *Journal of Advanced Research in Fluid Mechanics and Thermal Sciences* 5, no. 1 (2015): 8-23.
[25] Sahak, Ahmad Sofianuddin A., Nor Azwadi Che Sidik, and Siti Nurul Akmal Yusof. "A Brief Review of Particle Dispersion of Cavity Flow." *Journal of Advanced Research in Applied Sciences and Engineering Technology* 20, no. 1 (2020): 27-41. https://doi.org/10.37934/araset.20.1.2741
[26] Gomaa, Mona, and Tamer Kasem. "Simulation of Water Wave Interaction with Large Submerged Square Obstacles." *Journal of Advanced Research in Fluid Mechanics and Thermal Sciences* 86, no. 1 (2021): 14-26. https://doi.org/10.37934/arfmts.86.1.1426
[27] Waskito, Kurniawan Teguh. "On the High-Performance Hydrodynamics Design of a Trimaran Fishing Vessel." *Journal of Advanced Research in Fluid Mechanics and Thermal Sciences* 83, no. 1 (2021): 17-33. https://doi.org/10.37934/arfmts.83.1.1733
[28] CENPES *"Technical Specification - Metocean Data" PETROBRAS S.A* (2005).
[29] Utomo, Allessandro Setyo Anggito, M. F. Tjiptadi, and M. N. Luthfi. "Variations in The Distance Between Hulls that Affect the Resistance of The Floating Pontoon N219." *Journal of Advanced Research in Fluid Mechanics and Thermal Sciences* 83, no. 2 (2021): 127-134. https://doi.org/10.37934/arfmts.83.2.127134
[30] Menter, Florian R. "Two-equation eddy-viscosity turbulence models for engineering applications." *AIAA journal* 32, no. 8 (1994): 1598-1605. https://doi.org/10.2514/3.12149
[31] Hirt, Cyril W., and Billy D. Nichols. "Volume of fluid (VOF) method for the dynamics of free boundaries." *Journal of computational physics* 39, no. 1 (1981): 201-225. https://doi.org/10.1016/0021-9991(81)90145-5
[32] Eldeen, Ali Shehab Shams, Ahmed MR El-Baz, and Abdalla Mostafa Elmarhomy. "CFD Modeling of Regular and Irregular Waves Generated by Flap Type Wave Maker." *Journal of Advanced Research in Fluid Mechanics and Thermal Sciences* 85, no. 2 (2021): 128-144. https://doi.org/10.37934/arfmts.85.2.128144
[33] Naiem, Mohd Azzeri Md, Eizul Hanis Omar, Adi Maimun, Arifah Ali, Philip Wilson, Mohd Zarhamdy Md Zain, and Faizul Amri Adnan. "Drag analysis of three rudder-shaped like bodies." *Journal of Advanced Research in Fluid Mechanics and Thermal Sciences* 78, no. 1 (2021): 11-22. https://doi.org/10.37934/arfmts.78.1.1122